ARTICLE

doi:10.1038/nature12266

Combinatorial temporal patterning in progenitors expands neural diversity

Omer Ali Bayraktar[1,2] & Chris Q. Doe[1,2,3]

Human outer subventricular zone (OSVZ) neural progenitors and *Drosophila* type II neuroblasts both generate intermediate neural progenitors (INPs) that populate the adult cerebral cortex or central complex, respectively. It is unknown whether INPs simply expand or also diversify neural cell types. Here we show that *Drosophila* INPs sequentially generate distinct neural subtypes, that INPs sequentially express Dichaete, Grainy head and Eyeless transcription factors, and that these transcription factors are required for the production of distinct neural subtypes. Moreover, parental type II neuroblasts also sequentially express transcription factors and generate different neuronal/glial progeny over time, providing a second temporal identity axis. We conclude that neuroblast and INP temporal patterning axes act together to generate increased neural diversity within the adult central complex; OSVZ progenitors may use similar mechanisms to increase neural diversity in the human brain.

Proper brain development requires the production of a vast array of neurons and glia from a relatively small pool of stem/progenitor cells. Spatial patterning mechanisms generate progenitor diversity along the anterior–posterior and dorso–ventral axes, but the temporal patterning cues used by individual progenitors to make different neural cell types over time remain poorly characterized[1,2]. *Drosophila* neural progenitors (known as neuroblasts) are a model system to study temporal patterning. Most embryonic and larval neuroblasts undergo a 'type I' cell lineage to bud off a series of smaller ganglion mother cells (GMCs) that each make a pair of neurons or glia[3–8] (Fig. 1a), and transcription factors that specify temporal identity have been characterized in both embryonic neuroblasts[3–9] and larval neuroblasts[10,11].

We and others have recently discovered six 'type II' neuroblasts in the dorsomedial larval brain lobe (DM1–DM6) and two with more lateral positions[12–14] (Fig. 1a). Type II neuroblasts undergo self-renewing asymmetric cell divisions to generate a series of smaller INPs; then each INP also undergoes self-renewing divisions to generate a series of ~six GMCs, which typically each produce two neurons or glia[12–14] (Fig. 1a). Thus, both neuroblasts and INPs generate a series of progeny over time. For clarity, we state that type II neuroblasts transition from early to late over time, and INPs transition from young to old over time (Fig. 1a). Type II neuroblasts give rise to large clones of neurons and glia that populate the *Drosophila* adult brain central complex (CCX)[15–17]. Thus, type II neuroblasts share features with human OSVZ progenitors: both progenitors generate INPs, and both are used to increase the number of neurons in a particular brain region[18,19]. Although there are at least 60 morphologically distinct neurons in the fly adult CCX[20], we know virtually nothing about how parental neuroblasts or INPs generate neural diversity.

INPs sequentially express three transcription factors

We asked whether single INPs sequentially express a series of transcription factors, which would be indicative of temporal patterning. We used the previously characterized *R9D11-gal4* line driving the *UAS-GFP* construct to mark all INPs and their progeny from the DM1–DM6 neuroblast lineages[15] (Fig. 1b). INPs can be identified as small Deadpan $(Dpn)^+$ green fluorescent protein $(GFP)^+$ cells that are adjacent to the Dpn^+ GFP^- type II neuroblast (Fig. 1b); they are distinct from Dpn^- GMCs and neurons. Importantly, the age of an INP can be determined by its distance from the parental type II neuroblast: newly born young INPs are close to the parental neuroblast, whereas older INPs are displaced further away[13,15,21] (Fig. 1b). The ability to identify progressively older INPs allowed us to screen for transcription factors that were only present in young, middle or old INPs.

We screened a collection of 60 antibodies to neural transcription factors (Supplementary Table 1), and found three that were sequentially expressed in INPs. In late larvae at 96 h and 120 h after larval hatching (ALH), young INPs near the parental neuroblast contained the SOX-family transcription factor Dichaete (D)[22,23]; D was not detected in old INPs further from the parental neuroblast (DM3 shown in Fig. 1c, d; similar expression was observed in other dorsomedial lineages; Supplementary Fig. 1). By contrast, the Pax6 transcription factor Eyeless (Ey)[24] was detected in old INPs but not young D^+ INPs; there were very few double-negative or double-positive INPs (Fig. 1c, d). Similarly, the *R12E09-gal4* line containing a 2.7-kilobase (kb) *D* enhancer fragment[25] was expressed in young INPs, whereas the *OK107-gal4* enhancer trap at the *ey* locus[26] was expressed in old INPs (detailed expression patterns are shown in Supplementary Fig. 2; henceforth called $R12E09^D$ and $OK107^{ey}$). The D-to-Ey series was detected in all type II lineages examined and at all larval stages (DM1–DM6 at 24–120 h ALH; Fig. 1f, Supplementary Tables 2 and 3 and Supplementary Fig. 1). Thus, all INPs—from different type II neuroblasts and from early or late neuroblasts—sequentially express D and Ey (Fig. 1h, i).

In addition, we found that 'middle-aged' INPs contained the CP2-family DNA-binding factor Grainy head (Grh)[27]. Grh was assigned to middle-aged INPs because its expression overlapped both D and Ey at their expression border (Fig. 1e). Thus, INPs transition through four molecular states (Fig. 1h, g); it is likely that several GMCs are born during each of these windows, but for simplicity only one GMC per window is shown in our summaries. The D-to-Grh-to-Ey series was observed in INPs born from multiple type II neuroblasts (DM2–DM6; DM1 does not have detectable Grh) and in INPs born at all larval stages (Fig. 1g, Supplementary Tables 4 and 5 and Supplementary Fig. 1).

[1]Howard Hughes Medical Institute, University of Oregon, Eugene, Oregon 97403, USA. [2]Institute of Molecular Biology, University of Oregon, Eugene, Oregon 97403, USA. [3]Institute of Neuroscience, University of Oregon, Eugene, Oregon 97403, USA.

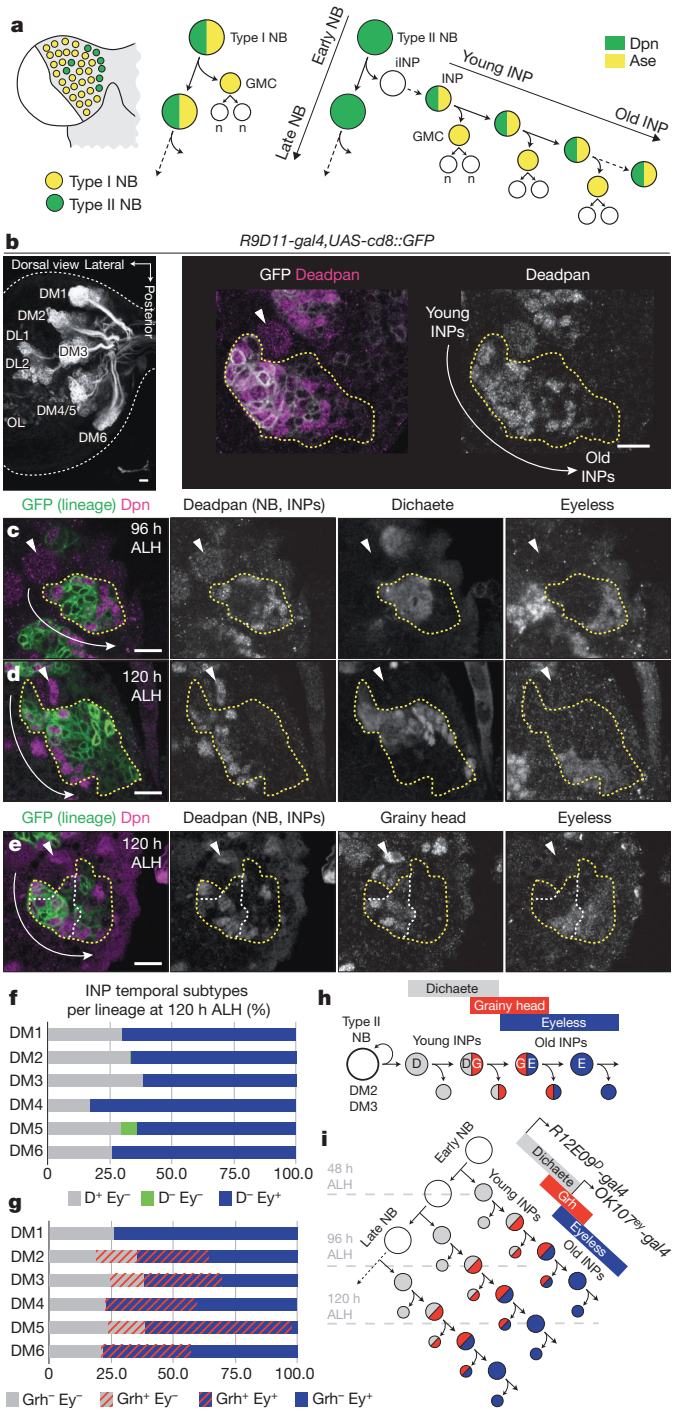

Figure 1 | INPs sequentially express candidate temporal identity factors. **a**, Position of type II neuroblasts (NB) (left). Cell lineage of type I and II neuroblasts (right). iINP, immature INP; n, neurons. **b**, Left, type II neuroblast lineages in one brain lobe (OL, optic lobe), *z*-projection, *R9D11-gal4 UAS-cd8::GFP*. Right, high magnification view of the DM3 lineage showing the parental neuroblast (Dpn^+ GFP^-, arrowhead), the smaller INPs (Dpn^+ GFP^+), and GMCs/neurons (Dpn^- GFP^+). Yellow line surrounds GFP^+ cells. **c**, **d**, **f**, Dichaete marks young INPs and Eyeless marks old INPs; DM3 lineage shown. *R9D11-gal4 UAS-cd8::GFP* marks INPs and their progeny (yellow line). **f**, Quantification. $n = 6$ brains, lineages in a single lobe counted, percentages per each lineage were averaged. **e**, **g**, Grainy head marks middle-aged INPs, which include the oldest $Dichaete^+$ INPs and the youngest $Eyeless^+$ INPs; DM3 lineage shown. *R9D11-gal4 UAS-cd8::GFP* marks INPs and their progeny (yellow line) and Grainy $head^+$ cells (white line). In addition, Grh^+ GFP^- immature INPs are observed between the parental neuroblast and the GFP^+ INP pool. **g**, Quantification as in **f**. **h**, **i**, Summary of Dichaete, Grainy head and Eyeless sequential expression in INPs. Gal4 lines expressed in INPs are indicated. Scale bars, 10 μm.

In addition to its expression in INPs, Grh is also detected in type II neuroblasts and transiently in immature INPs[28] (Fig. 1e). We conclude that most INPs progress through a stereotyped D-to-Grh-to-Ey transcription factor series (Fig. 1h, i).

Cross-regulation between INP transcription factors

We next wanted to determine whether D, Grh and Ey exhibit cross-regulation in INPs. We used *wor-gal4, ase-gal80* (ref. 29) to drive $UAS\text{-}D^{RNAi}$ in a *Dichaete* heterozygous background (subsequently called *D* RNAi, in which RNAi denotes RNA interference), which removed detectable D from INP lineages (Supplementary Fig. 4). Compared to wild type, *D* RNAi resulted in a significant loss of early born Grh^+ Ey^- INPs (Fig. 2a–d), without altering the number of later-born Grh^+ Ey^+ INPs (Fig. 2c and Supplementary Fig. 4). The same result was observed in *D* mutant clones (Supplementary Fig. 4). By contrast, misexpression of D did not lead to ectopic Grh expression (Supplementary Fig. 4). Thus, D is necessary for the timely activation of Grh in INP lineages, although D-independent inputs also exist (Fig. 2m).

To test whether Grh regulates D or Ey, we used *R9D11-gal4* to drive $UAS\text{-}grh^{RNAi}$ in a *grh* heterozygous background (subsequently called *grh* RNAi), which significantly reduced Grh levels in middle-aged INPs (Supplementary Fig. 5). *grh* RNAi increased the number of D^+ INPs at the expense of Ey^+ INPs (Fig. 2e, f) without altering the total number of INPs (control 33.2 ± 5.1; *grh* RNAi 31.7 ± 3.3; $P = 0.57$). As expected, *grh* RNAi did not change the numbers of D^+ and Ey^+ INPs in the DM1 lineage, which lacks Grh expression (Supplementary Fig. 5), nor did misexpression of Grh lead to ectopic Ey expression (Supplementary Fig. 5). We conclude that Grh represses D and activates Ey within INP lineages (Fig. 2m).

To determine whether Ey regulates D or Grh, we used $R12E09^D\text{-}gal4$ *UAS-FLP actin-FRT-stop-FRT-gal4* to drive permanent expression $UAS\text{-}ey^{RNAi}$ within INPs (subsequently called $R12E09^D \gg act\text{-}gal4$ or INP-specific *ey* RNAi; see Fig. 3a for summary). We confirmed that INP-specific *ey* RNAi removed Ey expression from INPs (Fig. 2g and Supplementary Fig. 7), without affecting Ey in the mushroom body or optic lobes (Supplementary Fig. 6). *ey* RNAi resulted in a notable increase in the number of old D^- Grh^+ INPs, without affecting the number of young D^+ INPs (Fig. 2g, h and Supplementary Fig. 7). Conversely, Ey misexpression in INPs significantly reduced the number of Grh^+ INPs (Fig. 2i, j and Supplementary Fig. 7) without altering the total number of INPs (control 31.7 ± 2.5; Ey misexpression 34.7 ± 3.4; $P = 0.11$). We also observed an increase in D^+ INPs (Fig. 2j and Supplementary Fig. 7), consistent with a regulatory hierarchy in which Ey represses Grh, which represses D. This effect was not due to ectopic Ey directly activating D because misexpression of Ey had no effect on D^+ INP numbers in the DM1 lineage, which lacks Grh expression (Supplementary Fig. 7). We conclude that Ey is necessary and sufficient to terminate the Grh expression window in INPs. We propose a 'feedforward activation/feedback repression' model for D-to-Grh-to-Ey cross-regulation (Fig. 2m).

We noticed that *ey* RNAi resulted in an increase in the total number of INPs. This could be due to a prolonged INP cell lineage, or to INPs switching to symmetric cell divisions that expand the INP population. To distinguish between these alternatives, we induced permanently marked clones using the mosaic analysis with a repressible cell marker (MARCM) technique[30] within wild-type and *ey* RNAi INPs at 24 h ALH, and assayed them at the end of larval life (120 h ALH) to determine whether they maintained a single INP per clone. Wild-type clones never contained an INP, showing that the INP lineages have ended by this time (Fig. 2k), whereas *ey* RNAi always contained a single INP within the clone (Fig. 2l). In addition, all Grh^+ INPs exhibited normal

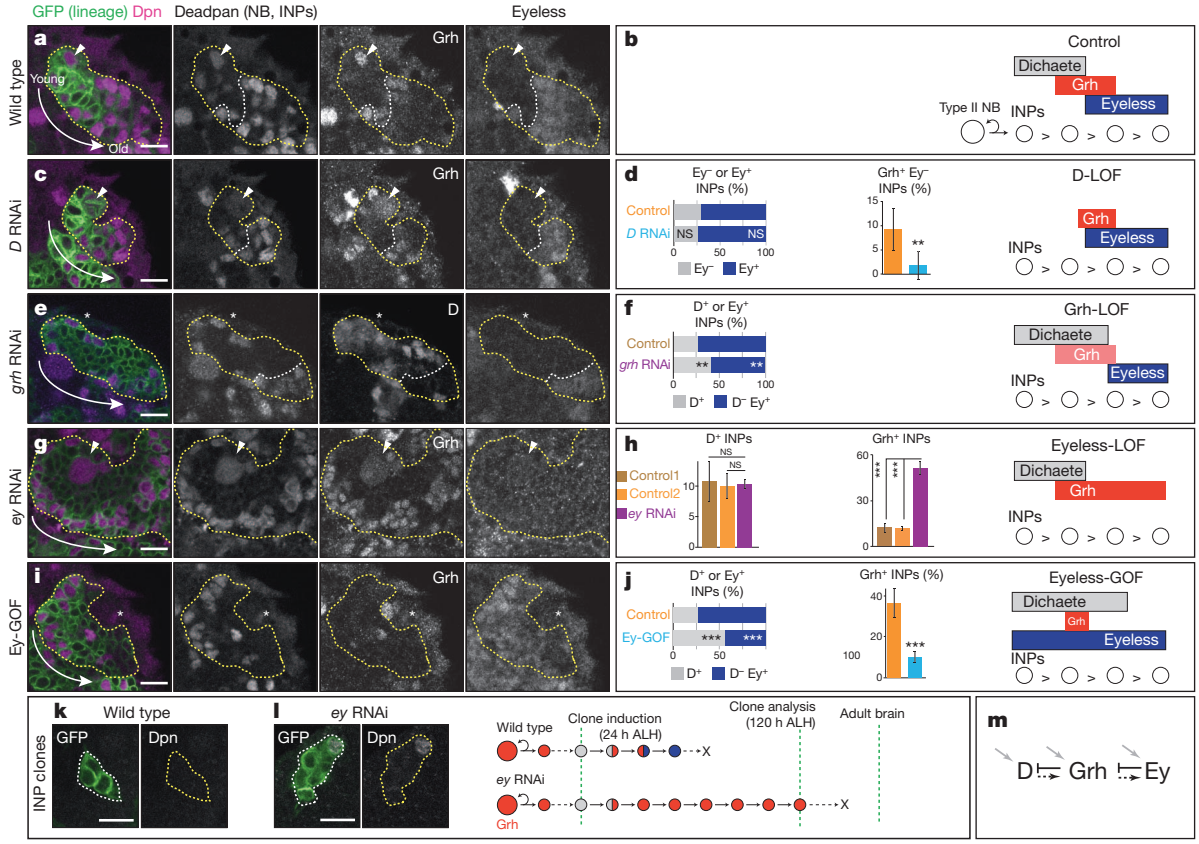

Figure 2 | Cross-regulation between INP temporal transcription factors. **a**, **c**, **e**, **g**, **i**, INP temporal transcription factor expression in DM2 lineage at 120 h ALH. INPs were marked with GFP (yellow outline) driven by: *wor-gal4 ase-gal80* (**a**, **c**), *R9D11-gal4* (**e**, **i**), or *R12E09^{D}-gal4* (**g**). See Methods for full genotypes. White line denotes the Ey border. Parental type II neuroblasts are marked by an arrowhead, or an asterisk when out of focal plane. **a**, **b**, Wild-type expression of Grh and Ey in INPs. **c**, **d**, *D* RNAi delays Grh expression in INPs, such that no Grh^{+} Ey^{-} INPs are observed. For Ey, see Supplementary Fig. 4a, b. Quantification of Ey^{+} and Grh^{+} Ey^{-} INP number is in **d** ($n = 6$). LOF, loss-of-function. **e**, **f**, *grh* RNAi extends D expression and delays Ey expression in INPs ($n \geq 5$). **g**, **h**, *ey* RNAi extends Grh expression in INPs ($n \geq 4$). GOF, gain-of-function. **i**, **j**, Ey misexpression reduces Grh expression in INPs ($n \geq 5$). **k**, **l**, *ey* RNAi extends the INP cell lineage. **k**, Wild-type MARCM clones induced early in single INPs never contain an INP at the end of larval life. **l**, *ey* RNAi MARCM clones maintain a single INP at the end of larval life ($n \geq 10$ clones). **m**, Summary. Black arrows, positive regulation; black T-bars, negative regulation; grey arrows, external positive regulation. Scale bars, 10 μm. All data represent mean ± s.d. NS, not significant. $^{**}P < 0.01$; $^{***}P < 0.001$.

INP markers (Dpn^{+} Ase^{+} nuclear Pros^{-}) and retained the ability to generate nuclear Pros^{+} Elav^{+} neurons (Supplementary Fig. 8). We conclude that *ey* RNAi extends individual INP cell lineages beyond that of wild-type INPs.

INPs generate different neurons and glia over time

Next, we asked next whether distinct neuronal or glial subtypes were generated during each transcription factor expression window. To determine the cell types produced by young D^{+} INPs or old Ey^{+} INPs, we used permanent lineage tracing (see Fig. 3a). Cells labelled by *R12E09^{D}* but not *OK107^{ey}* are generated by young INPs, whereas cells labelled by *OK107^{ey}* are generated by old INPs (Fig. 3b, e and Supplementary Fig. 3). We screened our collection of 60 transcription factor antibodies and found two that labelled subsets of young INP progeny, and two that labelled subsets of old INP progeny. The transcription factors D and Brain-specific homeobox (Bsh)[31] labelled sparse, non-overlapping subsets of young INP progeny (Fig. 3c, d), but not old INP progeny (Fig. 3f, g, j and Supplementary Fig. 9). Thus, young INPs generate Bsh^{+} neurons, D^{+} neurons, and many neurons that express neither gene. By contrast, the glial transcription factor Reverse polarity (Repo)[16,32,33] and the neuronal transcription factor Twin of eyeless (Toy)[34] labelled sparse, non-overlapping subsets of old INP progeny, but not young INP progeny (Fig. 3h–j and Supplementary Fig. 9). Additional mechanisms must restrict each marker (D, Bsh, Repo and Toy) to small subsets of young or old INP progeny; for example, each population could arise from just early or late born INPs within a type II neuroblast lineage (see below). We conclude that INPs sequentially express the D, Grh and Ey transcription factors, and they generate distinct neuronal and glial cell types during successive transcription factor expression windows (Fig. 3k). To our knowledge, these data provide the first evidence in any organism that INPs undergo temporal patterning.

INP factors specify temporally distinct neural subtypes

We wanted to determine whether D, Grh and Ey act as temporal identity factors that specify the identity of INP progeny born during their window of expression. First, we investigate the role of Ey in the specification of late born INP progeny. INP-specific *ey* RNAi resulted in the complete loss of the late born Toy^{+} neurons and Repo^{+} neuropil glia, but did not alter the number of early born D^{+} and Bsh^{+} neurons (Fig. 4a–i). Removal of Toy^{+} neurons (using *toy* RNAi) does not alter the number of Repo^{+} glia, and conversely removal of Repo^{+} glia (using *gcm* RNAi) does not alter the number of Toy^{+} neurons (Supplementary Fig. 10); thus Ey is independently required for the formation of both classes of late INP progeny. Conversely, permanent misexpression of Ey in early INPs increased late born Toy^{+} neurons and decreased early born Bsh^{+} neurons (Fig. 4j–n), consistent with Ey specifying late INP temporal identity. Unexpectedly, ectopic Ey reduced the number of late born Repo^{+} glia (Fig. 4n and Supplementary Fig. 11). We conclude that Ey is an INP temporal identity factor that promotes the independent specification of late born Toy^{+} neurons and Repo^{+} glia (Fig. 4o).

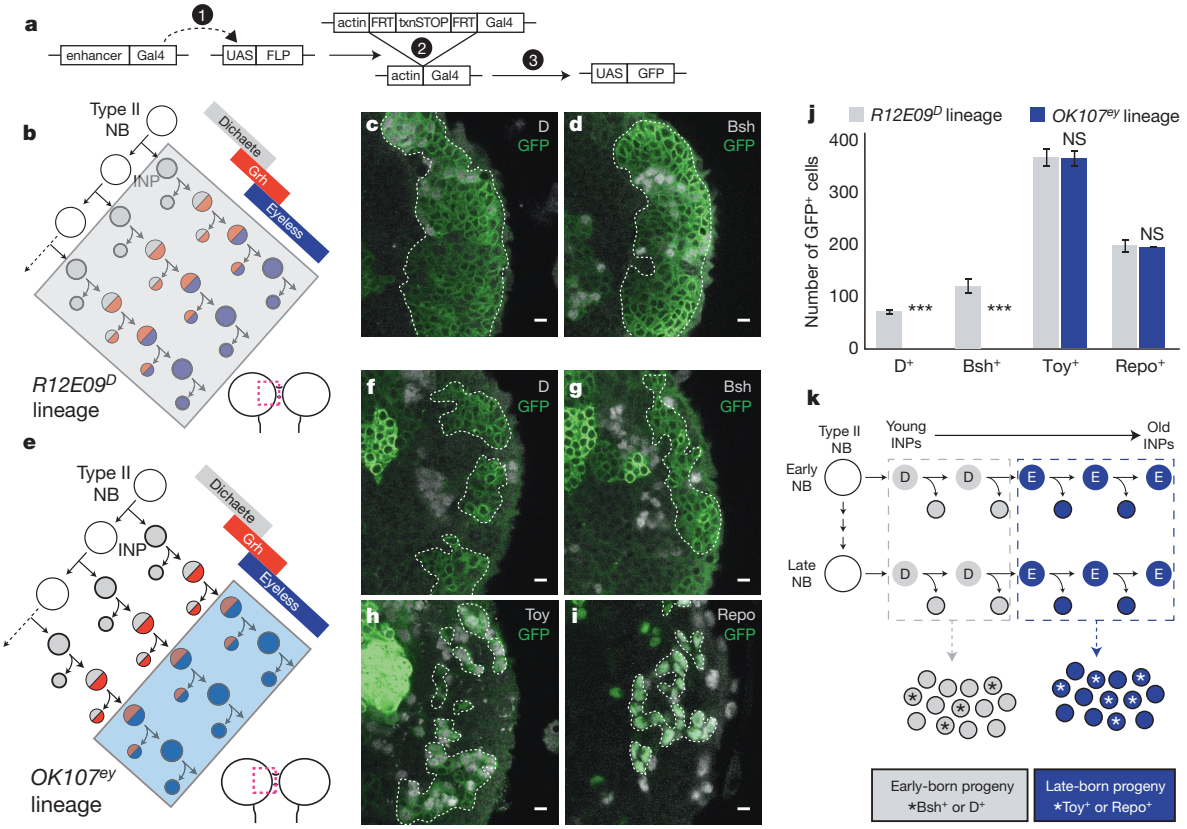

Figure 3 | INPs sequentially generate distinct temporal identities. **a**, Genetics of permanent lineage tracing. **b–d**, Permanent lineage tracing of all INP progeny using *R12E09^{D}-gal4*. Summary of GFP expression (**b**) and expression of D and Bsh in the GFP^{+} INP progeny (**c**, **d**). Dashed line surrounds GFP^{+} cells. **e–i**, Permanent lineage tracing of old INP progeny using the late INP *OK107^{ey}-gal4* line. Summary of GFP expression (**e**); D^{+} and Bsh^{+} neurons are excluded from late INP progeny (**f**, **g**), whereas Toy^{+} neurons and Repo^{+} glia are among the late born INP progeny (**h**, **i**); dashed line surrounds GFP^{+} cells. **j**, **k**, Quantification (**j**) and summary (**k**). GFP^{+} INP progeny in DM1–6 lineages were counted; $n \geq 3$ brain lobes for each marker. Region of dorsomedial brain imaged at 120 h ALH (boxed in cartoon). Scale bars, 5 μm. All data represent mean ± s.d. ***$P < 0.001$.

We next tested whether D and Grh specify early and mid INP temporal identity. INP-specific *D* RNAi led to a small but significant reduction in the number of early born Bsh^{+} neurons (Supplementary Fig. 11), whereas INP-specific *grh* RNAi severely reduced the number of early born Bsh^{+} neurons (Supplementary Fig. 11) without impairing INP proliferation (Supplementary Fig. 5) or late INP progeny (Supplementary Fig. 11). This is consistent with the Bsh^{+} neurons deriving from the D^{+} Grh^{+} expression window. Interestingly, misexpression of D or Grh did not increase Bsh^{+} neuron numbers (Supplementary Fig. 11); perhaps D/Grh co-misexpression is required to generate Bsh^{+} neurons. We conclude that both D and Grh are required, but not sufficient, for the production of Bsh^{+} early INP progeny.

Late born INP progeny are required for CCX morphology

The function of early or late born INP progeny in adult brain development is unknown. Here we determine the role of late born INP neurons and glia in the development and function of the adult central complex (CCX), an evolutionarily conserved insect brain structure containing many type II neuroblast progeny[15–17]. The CCX consists of four interconnected compartments at the protocerebrum midline: the ellipsoid body, the fan-shaped body, the bilaterally paired noduli, and the protocerebral bridge; each of these compartments is formed by a highly diverse set of neurons[20,35]. First, we used permanent lineage tracing (*OK107^{ey} ≫ act-gal4 UAS-cd8:GFP*) to map the contribution of late born Ey^{+} INP progeny to the adult CCX. We detected cell bodies in the dorsoposterior region of the CCX (data not shown), and their axonal projections extensively innervated the entire ellipsoid body, fan-shaped body, and protocerebral bridge, with much weaker labelling of the paired noduli (Fig. 5a–d). We conclude that old INPs contribute neurons primarily to the ellipsoid body, fan-shaped bod and protocerebral bridge regions of the CCX. Second, we used INP-specific *ey* RNAi to delete the late born Toy^{+} neurons and Repo^{+} glia (see Fig. 4). Loss of late born INP progeny generated major neuroanatomical defects throughout the adult CCX: the ellipsoid body and paired noduli were no longer discernible, the fan-shaped body was enlarged, and the protocerebral bridge was fragmented (Fig. 5f–l; quantified in 5o; summarized in 5p). Subsets of this phenotype were observed after removal of Toy^{+} neurons or Repo^{+} glia (Fig. 5m–o and Supplementary Fig. 12), showing that they contribute to distinct aspects of the CCX. Previous studies have described similar or weaker morphological CCX defects in *ey* hypomorphs[36], *toy* mutants[34], and after broad glia ablation during larval stages[37]. In addition, we found that *ey* RNAi adults have relatively normal locomotion, but have a significant deficit in negative geotaxis (Fig. 5q and Supplementary Video 1). We conclude that Ey is a temporal identity factor that specifies late born neuron and glial identity, and that these late born neural cell types are essential for assembly of the adult central complex.

Combinatorial temporal patterning increases diversity

We have found that Bsh^{+} neurons and Repo^{+} glia are sparse within the total population of young and old INP progeny, respectively, indicating that other mechanisms must help to restrict the formation of these neural subtypes. One mechanism could be temporal patterning within type II neuroblast lineages.

To determine whether type II neuroblasts change their transcriptional profiles over time, we assayed known temporal transcription factors[3,5,10,11,38] for expression in type II neuroblasts at five time points in their lineage (24, 48, 72, 96 and 120 h ALH). We observed no type II

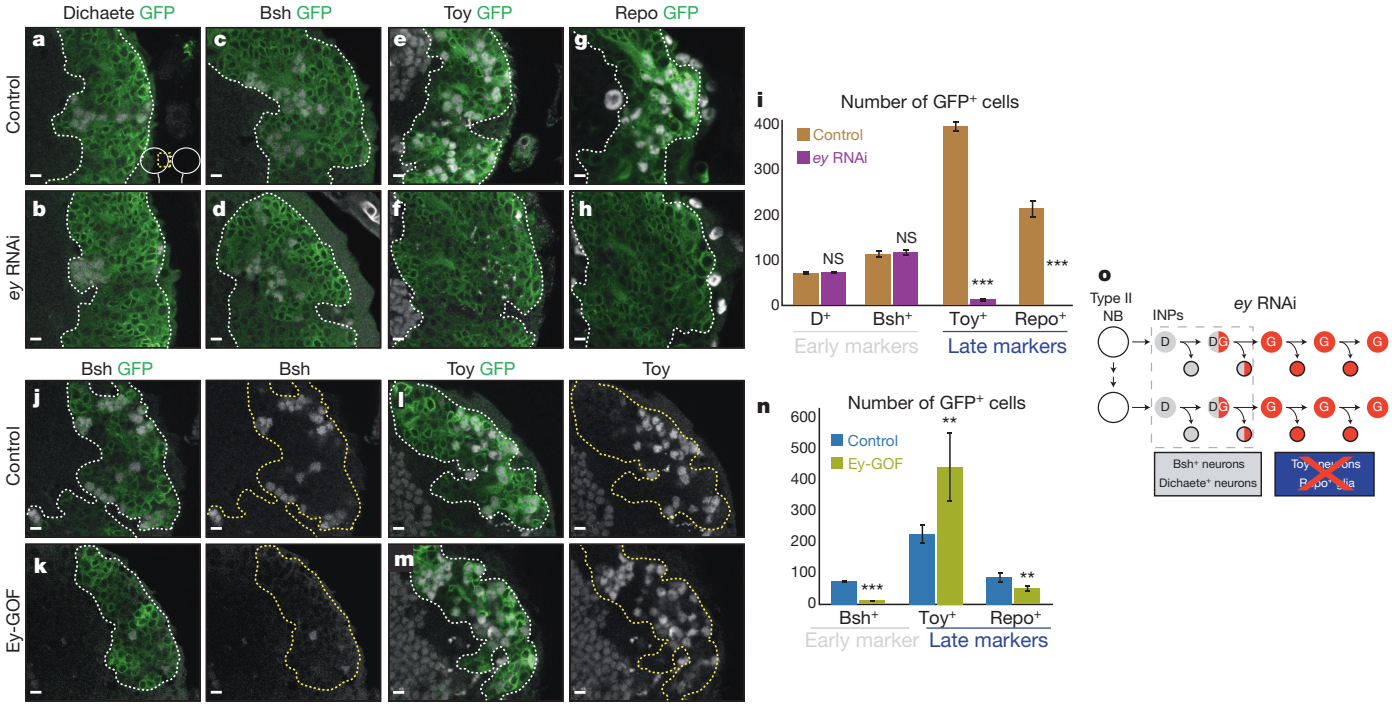

Figure 4 | Eyeless is a temporal identity factor for late born INP progeny. **a**–**i**, *ey* RNAi in INP lineages does not affect early born INP progeny (**a**–**d**), but eliminates late born Toy$^+$ neurons (**e**, **f**) and Repo$^+$ neuropil glia (**g**, **h**). Quantification ($n \geq 4$ brain lobes) in **i**. **j**–**n**, Ey misexpression in INP lineages leads to loss of early born Bsh$^+$ neurons (**j**, **k**), and increases the number of late born Toy$^+$ neurons (**l**, **m**). Quantification ($n \geq 5$) in **n**. **o**, Summary. Region of dorsomedial brain imaged at 120 h ALH (boxed in cartoon). G denotes Grh. Scale bars, 5 μm. All data represent mean ± s.d. $^{**}P < 0.01$; $^{***}P < 0.001$.

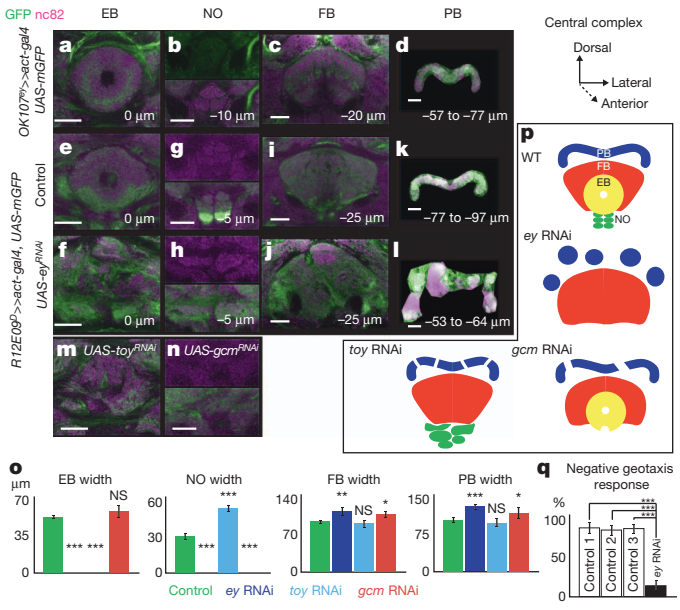

Figure 5 | Eyeless is required for adult brain central complex morphology and behaviour. **a**–**d**, Permanent lineage tracing of old INPs and their progeny (*OK107^{ey} ≫ act-gal4*) extensively labels the adult central complex. EB, ellipsoid body; FB, fan-shaped body; NO, noduli; PB, protocerebral bridge. **e**–**n**, *ey* RNAi (**f**–**l**), *toy* RNAi (**m**), or *gcm* RNAi (**n**) in INPs lineages produce distinct defects in CCX morphology. Adult brains, frontal view. The *z*-coordinates of single confocal sections are shown relative to ellipsoid body position. The protocerebral bridge was cropped out of the brain and displayed as a projection of indicated *z*-coordinates in **d**, **k** and **l**. Scale bars, 20 μm. **o**, Quantification of the width of CCX compartments ($n \geq 5$). **p**, Summary of CCX morphology after loss of late born INP progeny. **q**, *ey* RNAi flies have deficits in negative geotaxis. See Methods for controls. All data represent mean ± s.d. $^{*}P < 0.05$; $^{**}P < 0.01$; $^{***}P < 0.001$.

neuroblast expression for Hunchback, Kruppel, Pdm1/2 and Broad, and Grh was expressed in all type II neuroblasts at all time points. However, we identified three transcription factors with temporal expression in type II neuroblasts. D and Castor (Cas) were specifically detected in early type II neuroblasts: 3–4 neuroblasts at 24 h ALH, 0–1 neuroblast at 48 h ALH, and none later (Fig. 6a, b). Although we never detected D simultaneously in all type II neuroblasts at 24 h, permanent lineage tracing with *R12E09^D* labels all type II neuroblasts (Supplementary Fig. 3), indicating that all transiently express D. The third transcription factor, Seven up (Svp), showed a pulse of expression in a subset of type II neuroblasts at 48 h ALH, but was typically absent from younger or older type II neuroblasts (Fig. 6a, b). D, Cas and Svp are all detected in the anterior-most type II neuroblasts (probably corresponding to DM1–DM3), and thus at least these type II neuroblasts must sequentially express D or Cas, and Svp. We conclude that type II neuroblasts can change gene expression over time.

Next, we wanted to determine whether type II neuroblasts produce different INPs over time. We generated permanently labelled clones within the type II neuroblast lineages at progressively later time points (see Methods and Fig. 6c, d). If type II neuroblasts change over time to make different INPs, early and late neuroblast clones should contain different neural subtypes. We assayed clones for Repo$^+$ glia and Bsh$^+$ neurons, choosing these markers because Repo$^+$ neuropil glia have been proposed to be born early in type II neuroblast lineages[17] and Bsh$^+$ neurons were positioned far from the Repo$^+$ glia consistent with a different birth-order. Bsh$^+$ neuron numbers began to decline only in clones induced at the latest time point (Fig. 6e, g, i), showing that they are generated late in the type II neuroblast lineage (Fig. 6j, grey). By contrast, Repo$^+$ glia were detected in clones induced early but not late (Fig. 6f, h, i), proving that they are specifically generated by early type II neuroblasts (Fig. 6j, blue). This allows us to assign Repo$^+$ glia to an 'early neuroblast, old INP' portion of the lineage, and Bsh$^+$ neurons to a 'late neuroblast, young INP' portion of the lineage (Fig. 6j). We conclude that type II neuroblasts undergo temporal patterning, and

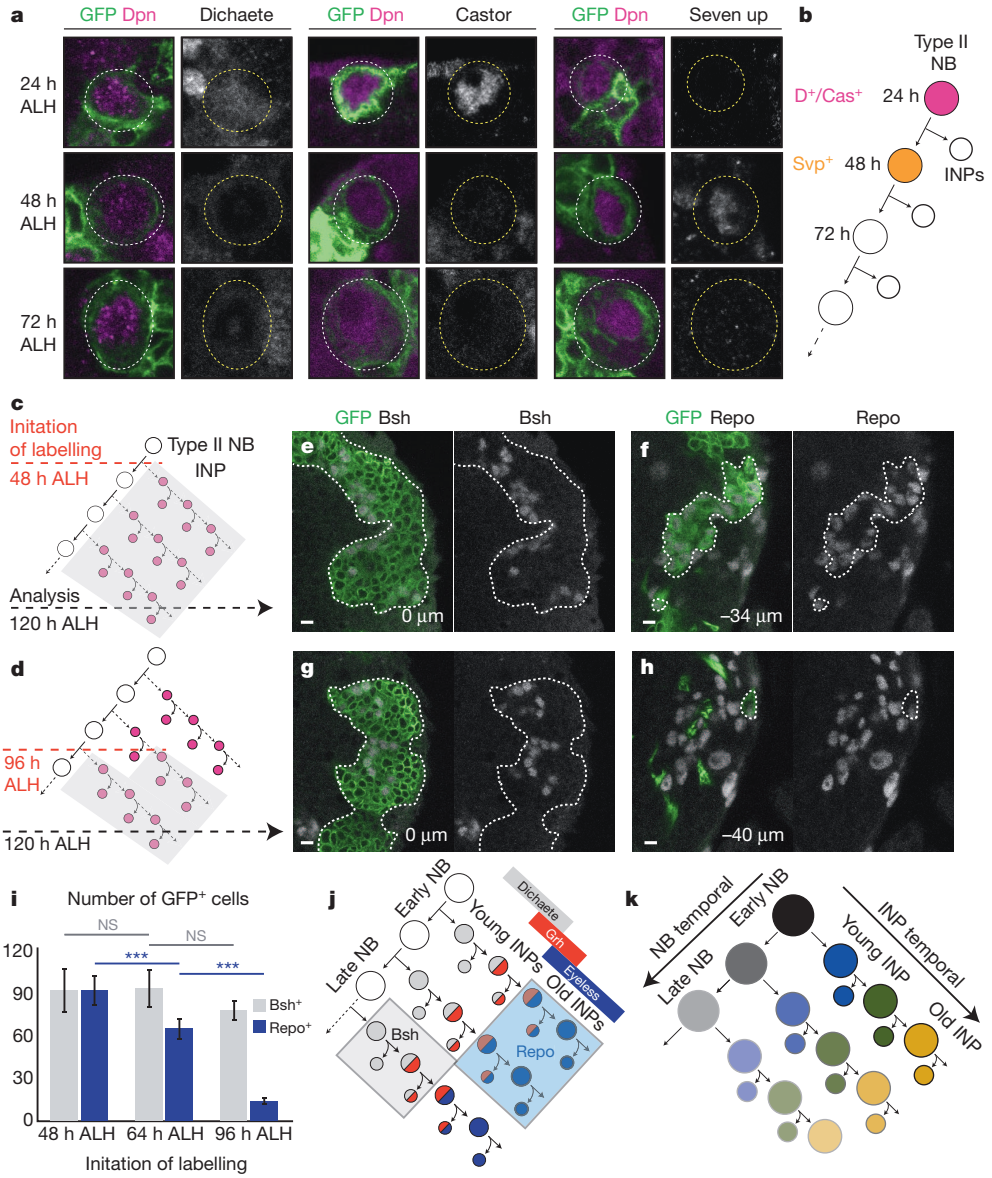

Figure 6 | INP temporal patterning acts combinatorially with neuroblast temporal patterning to increase neural diversity. **a**, **b**, Expression of D, Castor (Cas), and Seven up (Svp) in the anterior-most type II neuroblasts. Type II neuroblasts are identified with *pointed-gal4 UAS-GFP* (GFP; green) and Dpn (magenta). **c**, **d**, Schematics of INP permanent lineage tracing with $R12E09^{D}$*-gal4* induced at early (**c**) or late (**d**) larval stages; all time points analysed at 120 h ALH. Grey shading, labelled INP and progeny. **e**, **f**, Bsh^{+} neurons and $Repo^{+}$ glia are both marked by permanent labelling early in type II neuroblast lineages. Focal planes: Bsh, near neuroblast; Repo, further from the neuroblast (−34 µm). **g**, **h**, Bsh^{+} neurons, but not $Repo^{+}$ glia, are marked by permanent labelling late in type II neuroblast lineages. Focal planes: Bsh, near neuroblast; Repo, further from the neuroblast (−40 µm). Scale bars, 5 µm. **i**, Quantification. $n = 5$ for each time point. All data represent mean ± s.d. NS, not significant. $***P < 0.001$. **j**, Distinct neural progeny are born from early versus late type II neuroblast lineages. **k**, Neuroblast and INP temporal patterning act together to generate neural diversity.

propose that neuroblast temporal patterning acts together with INP temporal patterning to increase neural diversity in the adult brain (Fig. 6k).

Discussion

We have shown that INPs sequentially express three transcription factors (D, Grh and then Ey), and that different neural subtypes are generated from successive transcription factor windows. It is likely that multiple GMCs are born from each of the four known INP gene expression windows; GMCs born from a particular gene expression window may have the same identity, or may be further distinguished by 'subtemporal genes' as in embryonic type I neuroblast lineages[9]. We also show that each temporal factor is required for the production of a distinct temporal neural subtype. Loss of D or Grh leads to the loss of Bsh^{+} neurons; loss of Ey leads to loss of Toy^{+} neurons and $Repo^{+}$ glia, although the fate of the missing cells is unknown. An unexpected finding was that Ey limits the lifespan of INPs. Mechanisms that prevent INP de-differentiation have been characterized—loss of the translational repressor Brain tumour (Brat) or the transcription factor Earmuff (Erm) causes INPs to de-differentiate into tumorigenic type II neuroblasts[14,21]—but factors that terminate normal INP proliferation have never before been identified.

The D-to-Grh-to-Ey INP temporal identity factors are all used in other contexts during *Drosophila* development. Many embryonic neuroblasts sequentially express D and Grh[3]. Ey is expressed in mushroom body neuroblasts[39], and is required for development of the adult brain mushroom body[40]. Interestingly, mammalian orthologues of D and Ey (SOX2 and PAX6, respectively) are expressed in neural progenitors[41], including OSVZ progenitors[19], but have not been tested for a role in temporal patterning.

We have shown that there are two axes of temporal patterning within type II neuroblast lineages: both neuroblasts and INPs change over time to make different neurons and glia, thereby expanding neural diversity. It will be important to investigate whether INPs generated by OSVZ neural stem cells undergo similar temporal patterning (perhaps using SOX2 and PAX6), and whether combinatorial temporal patterning contributes to the neuronal complexity of the human neocortex.

METHODS SUMMARY

Larvae were staged to 120 h ALH based on age and morphology unless otherwise indicated; adult females were 3–5 days old. Immunohistochemistry was performed essentially as described[15] and imaged using Zeiss700/710 microscopes. INPs and GMC/neuronal progeny were distinguished by Dpn staining. *R12E09^{D} ≫ act-gal4* and the ubiquitously expressed temperature-sensitive Gal80 were used for inducible lineage tracing. Standard methods were used to assess geotaxis behaviour[42]. Data represent mean ± s.d. Two-tailed Student's *t*-tests were used. $*P < 0.05$; $**P < 0.01$; $***P < 0.001$.

Full Methods and any associated references are available in the online version of the paper.

Received 19 October 2012; accepted 1 May 2013.
Published online 19 June; corrected online 26 June 2013 (see full-text HTML version for details).

1. Tanabe, Y. & Jessell, T. M. Diversity and pattern in the developing spinal cord. *Science* **274,** 1115–1123 (1996).
2. Krumlauf, R. *et al.* Hox homeobox genes and regionalisation of the nervous system. *J. Neurobiol.* **24,** 1328–1340 (1993).
3. Maurange, C., Cheng, L. & Gould, A. P. Temporal transcription factors and their targets schedule the end of neural proliferation in *Drosophila*. *Cell* **133,** 891–902 (2008).
4. Brody, T. & Odenwald, W. F. Programmed transformations in neuroblast gene expression during *Drosophila* CNS lineage development. *Dev. Biol.* **226,** 34–44 (2000).
5. Isshiki, T., Pearson, B., Holbrook, S. & Doe, C. Q. *Drosophila* neuroblasts sequentially express transcription factors which specify the temporal identity of their neuronal progeny. *Cell* **106,** 511–521 (2001).
6. Tran, K. D. & Doe, C. Q. Pdm and Castor close successive temporal identity windows in the NB3–1 lineage. *Development* **135,** 3491–3499 (2008).
7. Grosskortenhaus, R., Robinson, K. J. & Doe, C. Q. Pdm and Castor specify late-born motor neuron identity in the NB7–1 lineage. *Genes Dev.* **20,** 2618–2627 (2006).
8. Grosskortenhaus, R., Pearson, B. J., Marusich, A. & Doe, C. Q. Regulation of temporal identity transitions in *Drosophila* neuroblasts. *Dev. Cell* **8,** 193–202 (2005).
9. Baumgardt, M., Karlsson, D., Terriente, J., Diaz-Benjumea, F. J. & Thor, S. Neuronal subtype specification within a lineage by opposing temporal feed-forward loops. *Cell* **139,** 969–982 (2009).
10. Zhu, S. *et al.* Gradients of the *Drosophila* Chinmo BTB-zinc finger protein govern neuronal temporal identity. *Cell* **127,** 409–422 (2006).
11. Kao, C. F., Yu, H. H., He, Y., Kao, J. C. & Lee, T. Hierarchical deployment of factors regulating temporal fate in a diverse neuronal lineage of the *Drosophila* central brain. *Neuron* **73,** 677–684 (2012).
12. Bello, B. C., Izergina, N., Caussinus, E. & Reichert, H. Amplification of neural stem cell proliferation by intermediate progenitor cells in *Drosophila* brain development. *Neural Dev.* **3,** 5 (2008).
13. Boone, J. Q. & Doe, C. Q. Identification of *Drosophila* type II neuroblast lineages containing transit amplifying ganglion mother cells. *Dev. Neurobiol.* **68,** 1185–1195 (2008).
14. Bowman, S. K. *et al.* The tumor suppressors Brat and Numb regulate transit-amplifying neuroblast lineages in *Drosophila*. *Dev. Cell* **14,** 535–546 (2008).
15. Bayraktar, O. A., Boone, J. Q., Drummond, M. L. & Doe, C. Q. *Drosophila* type II neuroblast lineages keep Prospero levels low to generate large clones that contribute to the adult brain central complex. *Neural Dev.* **5,** 26 (2010).
16. Viktorin, G., Riebli, N., Popkova, A., Giangrande, A. & Reichert, H. Multipotent neural stem cells generate glial cells of the central complex through transit amplifying intermediate progenitors in *Drosophila* brain development. *Dev. Biol.* **356,** 553–565 (2011).
17. Izergina, N., Balmer, J., Bello, B. & Reichert, H. Postembryonic development of transit amplifying neuroblast lineages in the *Drosophila* brain. *Neural Dev.* **4,** 44 (2009).
18. Fietz, S. A. *et al.* OSVZ progenitors of human and ferret neocortex are epithelial-like and expand by integrin signaling. *Nature Neurosci.* **13,** 690–699 (2010).
19. Hansen, D. V., Lui, J. H., Parker, P. R. & Kriegstein, A. R. Neurogenic radial glia in the outer subventricular zone of human neocortex. *Nature* **464,** 554–561 (2010).
20. Young, J. M. & Armstrong, J. D. Structure of the adult central complex in *Drosophila*: organization of distinct neuronal subsets. *J. Comp. Neurol.* **518,** 1500–1524 (2010).
21. Weng, M., Golden, K. L. & Lee, C. Y. dFezf/Earmuff maintains the restricted developmental potential of intermediate neural progenitors in *Drosophila*. *Dev. Cell* **18,** 126–135 (2010).
22. Russell, S. R., Sanchez-Soriano, N., Wright, C. R. & Ashburner, M. The *Dichaete* gene of *Drosophila melanogaster* encodes a SOX-domain protein required for embryonic segmentation. *Development* **122,** 3669–3676 (1996).
23. Nambu, P. A. & Nambu, J. R. The *Drosophila* fish-hook gene encodes a HMG domain protein essential for segmentation and CNS development. *Development* **122,** 3467–3475 (1996).
24. Halder, G., Callaerts, P. & Gehring, W. J. Induction of ectopic eyes by targeted expression of the *eyeless* gene in *Drosophila*. *Science* **267,** 1788–1792 (1995).
25. Pfeiffer, B. D. *et al.* Tools for neuroanatomy and neurogenetics in *Drosophila*. *Proc. Natl Acad. Sci. USA* **105,** 9715–9720 (2008).
26. Connolly, J. B. *et al.* Associative learning disrupted by impaired G_s signaling in *Drosophila* mushroom bodies. *Science* **274,** 2104–2107 (1996).
27. Uv, A. E., Thompson, C. R. & Bray, S. J. The *Drosophila* tissue-specific factor Grainyhead contains novel DNA-binding and dimerization domains which are conserved in the human protein CP2. *Mol. Cell. Biol.* **14,** 4020–4031 (1994).
28. Almeida, M. S. & Bray, S. J. Regulation of post-embryonic neuroblasts by *Drosophila* Grainyhead. *Mech. Dev.* **122,** 1282–1293 (2005).
29. Neumüller, R. A. *et al.* Genome-wide analysis of self-renewal in *Drosophila* neural stem cells by transgenic RNAi. *Cell Stem Cell* **8,** 580–593 (2011).
30. Lee, T. & Luo, L. Mosaic analysis with a repressible cell marker for studies of gene function in neuronal morphogenesis. *Neuron* **22,** 451–461 (1999).
31. Jones, B. & McGinnis, W. A new *Drosophila* homeobox gene, *bsh*, is expressed in a subset of brain cells during embryogenesis. *Development* **117,** 793–806 (1993).
32. Campbell, G. *et al.* RK2, a glial-specific homeodomain protein required for embryonic nerve cord condensation and viability in *Drosophila*. *Development* **120,** 2957–2966 (1994).
33. Xiong, W. C., Okano, H., Patel, N. H., Blendy, J. A. & Montell, C. *repo* encodes a glial-specific homeo domain protein required in the *Drosophila* nervous system. *Genes Dev.* **8,** 981–994 (1994).
34. Furukubo-Tokunaga, K., Adachi, Y., Kurusu, M. & Walldorf, U. Brain patterning defects caused by mutations of the *twin of eyeless* gene in *Drosophila melanogaster*. *Fly (Austin)* **3,** 263–269 (2009).
35. Hanesch, U., Fischbach, K. F. & Heisenberg, M. Neuronal architecture of the central complex in *Drosophila melanogaster*. *Cell Tissue Res.* **257,** 343–366 (1989).
36. Callaerts, P. *et al.* *Drosophila* Pax-6/eyeless is essential for normal adult brain structure and function. *J. Neurobiol.* **46,** 73–88 (2001).
37. Spindler, S. R., Ortiz, I., Fung, S., Takashima, S. & Hartenstein, V. *Drosophila* cortex and neuropile glia influence secondary axon tract growth, pathfinding, and fasciculation in the developing larval brain. *Dev. Biol.* **334,** 355–368 (2009).
38. Chai, P. C., Liu, Z., Chia, W. & Cai, Y. Hedgehog signaling acts with the temporal cascade to promote neuroblast cell cycle exit. *PLoS Biol.* **11,** e1001494 (2013).
39. Noveen, A., Daniel, A. & Hartenstein, V. Early development of the *Drosophila* mushroom body: the roles of eyeless and dachshund. *Development* **127,** 3475–3488 (2000).
40. Kurusu, M. *et al.* Genetic control of development of the mushroom bodies, the associative learning centers in the *Drosophila* brain, by the *eyeless*, *twin of eyeless*, and *Dachshund* genes. *Proc. Natl Acad. Sci. USA* **97,** 2140–2144 (2000).
41. Doe, C. Q. Neural stem cells: Balancing self-renewal with differentiation. *Development* **135,** 1575–1587 (2008).
42. Ali, Y. O., Escala, W., Ruan, K. & Zhai, R. G. Assaying locomotor, learning, and memory deficits in *Drosophila* models of neurodegeneration. *J. Vis. Exp.* **49,** e2504 (2011).

Supplementary Information is available in the online version of the paper.

Acknowledgements We thank L. Manning and K. Hirono for larval brain stains and imaging; S.-L. Lai, J. Eisen, T. Herman and B. Bowerman for comments on the manuscript; T. Carney and M. Miller for discussions; and the fly community for reagents. This work was supported by National Institutes of Health (NIH) grants T32HD216345 and T32GM007413 (to O.A.B.), NIH R01HD27056 (to C.Q.D.) and the Howard Hughes Medical Institute (to C.Q.D.).

Author Contributions O.A.B. performed the experiments; O.A.B. and C.Q.D. conceived of the project and wrote the manuscript.

Author Information Reprints and permissions information is available at www.nature.com/reprints. The authors declare no competing financial interests. Readers are welcome to comment on the online version of the paper. Correspondence and requests for materials should be addressed to C.Q.D. (cdoe@uoregon.edu).

METHODS

Fly stocks. The chromosomes and insertion sites of transgenes (if known) are shown next to genotypes. Unless indicated, lines were obtained from Bloomington stock centre (FlyBase IDs shown).

Enhancer Gal4 lines and reporters: *R9D11-gal4* (*III, attP2*) (ref. 25). *R9D11-gal4* (*II, attP40*) (ref. 43). *R12E09^{D}-gal4* (*III, attP2*) (ref. 25). *OK107^{ey}-gal4* (*IV*) (ref. 26). *R9D11-CD4-tdTom* (*III, attP2*) (ref. 44). *10XUAS-IVS-mCD8::GFP* (*III, su(Hw)attP2*) (ref. 9) (referred to as *UAS-GFP*), *Pointed-gal4$^{14\text{-}94}$* (*III*) (ref. 45).

Mutant stocks: *D^{87},FRT2A/Tm3,Sb* (ref. 23). *grh^{370}/CyO,actGFP* (ref. 46).

Transgenic RNAi: *UAS-D^{RNAi}* (II; VDRC, 107194). Lines from the TRiP collection (*III, attP2*): *UAS-grh^{RNAi}* (FBst0028820). *UAS-ey^{RNAi}* (FBst0032486). *UAS-toy^{RNAi}* (FBst0029346). *UAS-gcm^{RNAi}* (FBst0031518). TRiP RNAi controls: *y v; attP2* and *y sc v; UAS-mCherry^{RNAi}*. Other controls: *y w*, *w^{118}*, or *UAS-His2A::mRFP*.

Lineage tracing transgenes: *UAS-FLP* (*I*; FBst0008208 and *III*; FBst0008209). *actin-FRT-stop-FRT-gal4* (*I*; FBst0004779 and *III*; FBst0004780). *tub-gal80^{ts}* (*II*; FBst0007108).

Other: *UAS-D* (*II*) (FBst0008861). *UAS-grh* (*II*) (ref. 9). *UAS-ey* (*II*) (FBst0006294).

Recombinant chromosomes generated in this study: *R9D11-gal4, UAS-GFP* (*III*). *R12E09^{D}-gal4, UAS-GFP* (*III*). *UAS-FLP, actin-FRT-stop-FRT-gal4* (both *I* and *III*).

Fly genetics. Permanent lineage tracing, which involves the flippase (FLP)-mediated removal of a transcriptional stop cassette between the constitutive *actin* promoter and the *gal4* open reading frame, is summarized in Fig. 3a. For lineage tracing of young or old INP progeny (Figs 3 and 5), the *R12E09^{D}* or *OK107^{ey}* Gal4 lines were either crossed to *UAS-FLP, actin-FRT-stop-FRT-gal4;;UAS-GFP* (*I;;III*) for labelling with membrane localized GFP or to *UAS-FLP, ubi-FRT-stop-FRT-nGFP* (*II*) for labelling with nuclear GFP (G-TRACE)[47].

For driving expression of *UAS-RNAi* or misexpression transgenes, the following lines were used: *UAS-dcr2; wor-gal4, ase-gal80; UAS-mCD8::GFP* (ref. 29). *R9D11-gal4; R9D11-gal4, UAS-GFP (II, III). R12E09^{D} ≫ act-gal4* [*UAS-FLP, actin-FRT-stop-FRT-gal4;; R12E09^{D}-gal4, UAS-GFP/Tm6B* (*I;;III*)]. *R9D11 ≫ act-gal4* [*UAS-FLP, actin-FRT-stop-FRT-gal4;; R9D11-gal4, UAS-GFP* (*I;;III*)]. Below are the genotypes used in RNAi and misexpression experiments

D RNAi was driven by *wor-gal4 ase-gal80 UAS-dcr2* in *D^{87}*/+; control was *w^{1118}*. *grh* RNAi was driven by *R9D11-gal4, R9D11-gal4* in *grh^{370}*/+; control was *attP2* (empty transgene docking site). *ey* RNAi was driven by *R12E09^{D} ≫ act-gal4*; controls were (1) *attP2* and (2) *UAS-mCherry^{RNAi}*. Ey-GOF was driven by *R9D11-gal4 ≫ act-gal4*; control was *yw* or *UAS-His2A*::mRFP (for quantification of INP progeny). *toy* and *gcm* RNAi were driven by *R12E09^{D} ≫ act-gal4*.

For inducible lineage tracing (Fig. 6), *R12E09^{D} ≫ act-gal4* was combined with the ubiquitously expressed *tub-gal80^{ts}* so that temperature shifts were used to turn on labelling by *R12E09^{D}* at different points in the type II neuroblast lineages. *R12E09^{D}-gal4, UAS-GFP* flies were crossed to *tub-gal80^{ts}; UAS-FLP, actin-FRT-stop-FRT-gal4* (*II;III*). The newly hatched 0–6 h ALH larvae were reared at restrictive temperature at 18 °C for 72, 96 or 144 h (which correspond to 48, 64 and 96 h of development at 23 °C, respectively), then shifted to permissive temperature at 30 °C to induce labelling.

To generate wild-type or *D^{87}* type II NB MARCM clones, *hsFLP; tub-gal4, UAS-mCD8::GFP/CyO; tub-gal80, FRT2A/TM6C,Sb* flies were crossed to *FRT2A* or *D^{87},FRT2A/Tm3,Sb* flies respectively. To induce clones, 24 h ALH larvae were heat-shocked at 37 °C for 30 min, and reared to 120 h ALH. To generate wild-type or *ey* RNAi INP MARCM clones, *hsFLP; FRT40A, tub-gal80/CyO,actGFP; tub-gal4, UAS-mCD8::GFP/TM6B* flies were crossed to *FRT40A* or *FRT40A; UAS-ey^{RNAi}* flies respectively. To induce clones, 24 h ALH larvae were heat-shocked at 37 °C for 1 h, and reared to 120 h ALH. INP clones were identified in the dorsomedial brain as multicellular clones ($n > 3$ cells) without a neuroblast.

Unless indicated otherwise, larvae were staged to 120 h ALH based on age and morphology (late wandering larvae near pupariation) for dissections. For other time points, newly hatched 0–4 h ALH larvae were picked and reared accordingly. Adult females were aged to 3–5 days for dissections.

Immunohistochemistry. Primary antibodies were rat anti-Dpn (1:50, C.Q.D. laboratory), guinea pig anti-Dpn (1:2,000, J. Skeath), chicken anti-GFP (1:2,000, Aves Laboratories), guinea pig anti-D (1:500, J. Nambu), rabbit anti-D (1:500, J. Nambu), rabbit anti-Ey (1:3,500, U. Walldorf), rat anti-Grh (1:1,000, S. Thor), guinea-pig anti-Bsh (1:250, M. Sato), guinea-pig anti-Toy (1:500, U. Walldorf), mouse anti-Repo (1:4, DHSB), mouse anti-nc82 (1:100, DHSB), rabbit anti-DsRed (1:500, Clontech Laboratories), rabbit anti-Ase (1:2,000, C.-Y. Lee), mouse anti-Pros (MR1A, 1:1,000, C.Q.D. laboratory), rat anti-Elav (1:50, DHSB), rabbit anti-Cas (1:1,000, W. Odenwald), rat anti-Svp (1:500, T. Isshiki). Additional primary antibodies are listed in Supplementary Table 1. Secondary antibodies were from Molecular Probes or Jackson Immunoresearch.

Dissection and immunostaining were performed as described previously[15] with few modifications. Larval brains were fixed in 4% formaldehyde in PBST (1× PBS with 0.3% Triton X-100) for 25 min, rinsed, and blocked in PBST with 5% normal goat and donkey serum mix (Vector Laboratories) for 30 min. Adult brains were fixed in 4% formaldehyde in PBT (1× PBS with 1% Triton X-100), rinsed, and blocked in PBT plus 5% serum. Adult brains were incubated in primary antibodies for 2 days at 4 °C, then in secondary antibodies for 2 days at 4 °C. Brains were stored in Vectashield (Vector Laboratories). For EdU incorporation, dissected larval brains were incubated in S2 medium (Sigma) containing 100 μg ml^{-1} EdU (Molecular Probes) at 25 °C for 2 h. After completing standard fixation and antibody staining procedures, EdU was detected by following manufacturers protocols (Molecular Probes).

Imaging. Brains were mounted in Vectashield (Vector Laboratories). Images were captured with a ZeissLSM700 or LSM710 confocal microscope with a *z*-resolution of 1.0 μm, and processed in the open source software FIJI (http://fiji.sc) and Adobe Photoshop CS5. Figures were made in Adobe Illustrator CS5. Three-dimensional brain reconstructions were generated using Imaris software (Bitplane).

Quantification of INPs and progeny. INPs were labelled with cell-type specific Gal4-driven *UAS-mCD8::GFP* and distinguished from their GMC/neuronal progeny by Dpn staining. For the quantification of Grh expression in middle-aged INPs, newly mature INPs that show weak levels of Grh (inherited from immature INPs) were excluded. For the quantification of temporal identities, INP progeny were marked with permanent lineage tracing. GFP^{+} INP progeny in DM1–6 lineages were counted. GFP^{+} Repo^{+} glia in the lateral brain were also counted, see Supplementary Fig. 10. For better labelling of glia, nuclear localized GFP (nGFP) was used.

Negative geotaxis assays were performed as described previously[42]. Ten adults of each genotype (three-day-old virgin females) were placed in a vial at room temperature. Flies were allowed to acclimate for 1 min, and then gently tapped to the bottom of the vial. The number of flies that climbed above the vertical distance of 8 cm by 10 s after the tap was recorded as a percentage of total flies. Ten trials were conducted for each genotype, with a 1-min rest period between each trial. The results of ten trials were averaged and plotted as the negative geotaxis response. *ey* RNAi genotype was *R12E09^{D} ≫ act-gal4 UAS-ey^{RNAi}*. Controls were (1) *R12E09^{D} ≫ act-gal4 attP2*, (2) *R12E09^{D} ≫ act-gal4 UAS-mCherry^{RNAi}*, and (3) *no gal4 ≫ act-gal4 UAS-ey^{RNAi}*.

Statistics. Data represent mean ± s.d. Two-tailed Student's *t*-tests were used to assess statistical significance. $*P < 0.05$; $**P < 0.01$; $***P < 0.001$.

43. Pfeiffer, B. D. *et al.* Refinement of tools for targeted gene expression in *Drosophila*. *Genetics* **186,** 735–755 (2010).
44. Han, C., Jan, L. Y. & Jan, Y. N. Enhancer-driven membrane markers for analysis of nonautonomous mechanisms reveal neuron-glia interactions in *Drosophila*. *Proc. Natl Acad. Sci. USA* **108,** 9673–9678 (2011).
45. Zhu, S., Barshow, S., Wildonger, J., Jan, L. Y. & Jan, Y. N. Ets transcription factor Pointed promotes the generation of intermediate neural progenitors in *Drosophila* larval brains. *Proc. Natl Acad. Sci. USA* **108,** 20615–21620 (2011).
46. Uv, A. E., Harrison, E. J. & Bray, S. J. Tissue-specific splicing and functions of the *Drosophila* transcription factor Grainyhead. *Mol. Cell. Biol.* **17,** 6727–6735 (1997).
47. Evans, C. J. *et al.* G-TRACE: rapid Gal4-based cell lineage analysis in *Drosophila*. *Nature Methods* **6,** 603–605 (2009).